Electronic structure of oxysulfide (LaO)CuS and $(La_{1-x}Ca_xO)Cu_{1-x}Ni_xS$ ($x \leqslant 0.10$) studied by photoemission and inverse-photoemission spectroscopies

Hitoshi Sato,[1]* Hiroshi Negishi,[2] Asami Wada,[1] Akihiro Ino,[3] Saiko Negishi,[2] Chiyuki Hirai,[1] Hirofumi Namatame,[3] Masaki Taniguchi,[1,3] Koichi Takase,[4] Yumiko Takahashi,[4] Tomohiro Shimizu,[4] Yoshiki Takano,[4] and Kazuko Sekizawa[4]

[1]*Graduate School of Science, Hiroshima University, Kagamiyama 1-3-1, Higashi-Hiroshima 739-8526, Japan*

[2]*Department of Quantum Matter, ADSM, Hiroshima University, Kagamiyama 1-3-1, Higashi-Hiroshima 739-8530, Japan*

[3]*Hiroshima Synchrotron Radiation Center, Hiroshima University, Kagamiyama 2-313, Higashi-Hiroshima 739-8526, Japan*

[4]*College of Science and Technology, Nihon University, Kanda-Surugadai 1-8, Chiyoda-ku, Tokyo 101-8308, Japan*

(Received 12 November 2002; published 17 July 2003)

Valence-band and conduction-band electronic structure of the transparent *p*-type semiconductor (LaO)CuS and the Ca and Ni co-doped system $(La_{1-x}Ca_xO)Cu_{1-x}Ni_xS$ ($x \leqslant 0.10$) has been investigated by means of photoemission and inverse-photoemission spectroscopies. It is confirmed that the valence bands of (LaO)CuS are composed of the bonding and antibonding states of the Cu $3d$ (t_{2g}) and S $3p$ orbitals as well as the nearly localized Cu $3d$ (e_g), and the O $2p$ states. With increasing x up to $x=0.03$, the structure due to the Cu $3d$ (e_g) states shifts away from the Fermi level (E_F) and the energy separation between the valence-band maximum and conduction-band minimum decreases rapidly, followed by an appearance of new density of states (DOS) derived from the Ni $3d$ and S $3p$ states just above E_F of (LaO)CuS. For $x \geqslant 0.03$, the new DOS shows up with x, while the energy position of the Cu $3d$ (e_g)-derived structure no longer shifts. The finite DOS at E_F has been observed as a clear structure for $x=0.10$. These results are not understood in terms of a rigid-band model. We propose a different band model for $(La_{1-x}Ca_xO)Cu_{1-x}Ni_xS$ taking into account the Ni $3d$ and S $3p$-derived new DOS.

DOI: 10.1103/PhysRevB.68.035112 PACS number(s): 71.20.Nr, 79.60.−i

I. INTRODUCTION

Layered oxysulfide (LaO)CuS is known to be one of few materials with a transparent *p*-type semiconductive property. For the development of optoelectronic devices, fabrication of transparent *p*-*n* junctions based on wide-gap materials is essentially important. However, most transparent conductive materials are *n* type and a conversion to *p*-type conductors is, in general, difficult. Recently, (LaO)CuS is expected to be one of the candidate materials for optoelectronic devices in ultraviolet and/or blue regions, since it has a wide band-gap energy of ~3.1 eV,[1–3] with an intense photoluminescence due to the interband transition at room temperature.[3]

The crystal structure of (LaO)CuS shown in Fig. 1 is tetragonal (LaO)AgS type with a space group of $P4/nmm$,[4,5] and it consists of $[LaO]^{1+}$ and $[CuS]^{1-}$ layers with OLa_4 and CuS_4 tetrahedra, respectively, alternately stacked along the *c* axis. An interlayer interaction between the almost ionic LaO and covalent CuS layers is believed to be weak. The valence bands are primary composed of well-hybridized states of the Cu $3d$ and S $3p$ orbitals, while the bottom of the conduction bands mainly of the Cu $4s$ states, leading to semiconductive properties, as predicted by the recent band-structure calculation using the full-potential linearized augmented plane-wave (FLAPW) method.[1]

On the other hand, Sekizawa *et al.* have studied exhaustively the doping effect on the electrical and magnetic properties of (LaO)CuS. The Ca singly doped system $(La_{1-x}Ca_xO)CuS$ is all semiconductive up to the solubility limit of $x=0.15$,[6] while the Sr-doped system is semiconductive for $x<0.03$ and metallic for $x>0.03$.[2,7] In case of the Ca and Ni co-doped system $(La_{1-x}Ca_xO)Cu_{1-x}Ni_xS$, where the La and Cu ions are simultaneously substituted by the Ca and Ni ions, respectively, the resistivity decreases remarkably with x and its temperature dependence changes from semiconductive ($x<0.03$) to metallic ($x>0.03$) behaviors. In particular, a metal (low temperature)–semiconductor (high temperature) transition takes place at ~150 K for the critical concentration of $x=0.03$.[6,8] Moreover, a ferromagnetic behavior with a magnetic moment of $\sim 0.06\mu_B$/Ni atom is observed for $x \geqslant 0.01$ and the Curie temperatures are

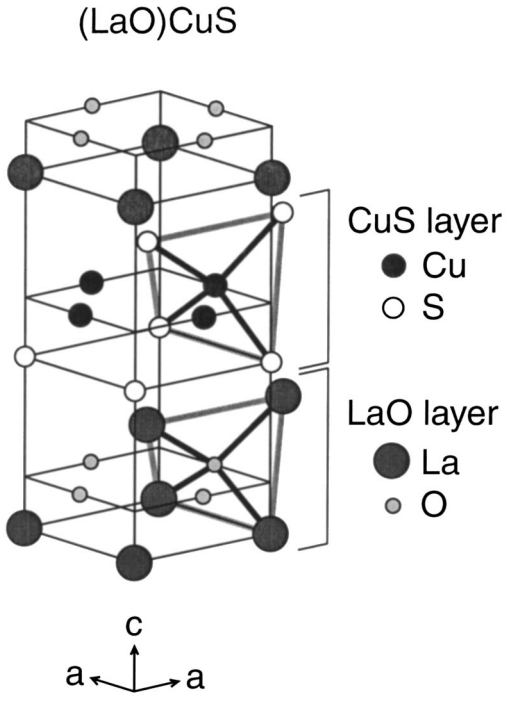

FIG. 1. Crystal structure of (LaO)CuS.

evaluated to be ~300 and ~380 K for $x=0.01$ and 0.10, respectively.

Most recently, nuclear magnetic resonance (NMR) measurements on $(La_{1-x}Ca_xO)Cu_{1-x}Ni_xS$ have revealed that the density of states (DOS) at the Fermi level (E_F) at the Cu sites is substantially low still for the metallic region though it slightly increases with x.[9] The ionic state of the Cu ion in (LaO)CuS ($x=0$) is monovalent (Cu^{1+}, $3d^{10}$) and the value of the ^{63}Cu NMR shift is almost independent of x. The x-ray photoemission spectroscopy (XPS) study, on the other hand, suggests the existence of the Cu^{2+} ($3d^9$) ions even for (LaO)CuS and an increase of the Cu^{2+} ions with x from the Cu $2p$ satellite intensity[8] in contrast to the NMR results.[9] For the Sr singly doped system $(La_{0.95}Sr_{0.05}O)CuS$ with a metallic behavior, ultraviolet photoemission spectroscopy (UPS), XPS and inverse-photoemission spectroscopy (IPES) have been performed.[1] The observed results are discussed compared with the calculated band structure of (LaO)CuS, neglecting any Sr-doping effect.

In the present study, we have investigated the valence-band and conduction-band electronic structure of (LaO)CuS and the Ca and Ni co-doped system $(La_{1-x}Ca_xO)Cu_{1-x}Ni_xS$ ($x\leqslant 0.07$) by means of UPS and IPES. The Ni substitutions within the CuS layer are expected to change the electronic structure more than the singly doped system. We have also carried out the XPS and synchrotron radiation photoemission (SRPES) experiments for $x=0$ and 0.10. Based on the experimental results, we discuss the variations of the valence bands and conduction bands by the co-doping effect and propose a band model of $(La_{1-x}Ca_xO)Cu_{1-x}Ni_xS$ taking into account the Ni $3d$ and S $3p$-derived states.

II. EXPERIMENT

The UPS and IPES spectra were taken using the UPS and PES spectrometers mounted in ultrahigh vacuum chambers with base pressures of 1×10^{-9} and 1×10^{-10} Torr, respectively. The UPS spectrometer is composed of an He discharge lamp ($h\nu=21.2$ and 40.8 eV) and a double-stage cylindrical-mirror analyzer (DCMA). Pass energy of photoelectrons was fixed to 16.0 eV with a corresponding energy resolution of 0.2 eV. The IPES spectrometer[10,11] is made up of the low-energy electron gun of Erdmann-Zipf type with a BaO cathod and a band-pass-type photon detector centered at $h\nu=9.43$ eV. The IPES spectra were measured with the bremsstrahlung isochromat spectroscopy mode with a total energy resolution of 0.56 eV.[10,11]

The SRPES experiments were carried out on the beamline BL7 at Hiroshima Synchrotron Radiation Center (HSRC). The synchrotron radiation generated from the storage ring, HiSOR, was monochromatized by the Dragon-type monochromator.[12] We used a photoemission spectrometer with the hemispherical photoelectron analyzer (GAMMA-DATA SCIENTA SES100) attached to the analysis chamber at the end station of BL7. The total-energy resolution of the SRPES spectra was ~100 meV around $h\nu=100$ eV. The XPS experiments were also done using the same analysis chamber at BL7 and photoelectrons were excited using the Mg K_α line ($h\nu=1253.6$ eV).

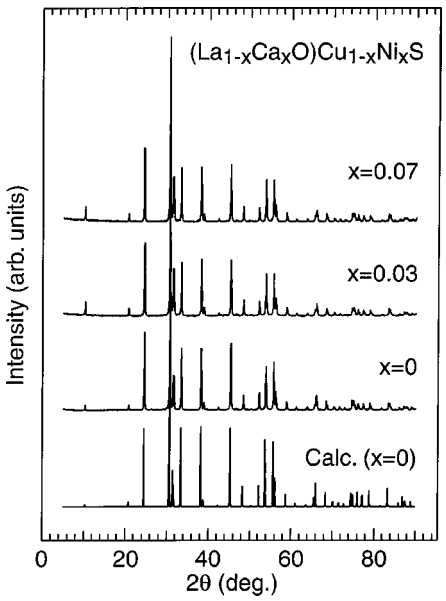

FIG. 2. XRD patterns of $(La_{1-x}Ca_xO)Cu_{1-x}Ni_xS$ with $x=0$, 0.03, and 0.07 together with the calculation for $x=0$. No peak due to impurities is observed.

All spectra were collected at room temperature for $(La_{1-x}Ca_xO)Cu_{1-x}Ni_xS$ polycrystals. Clean surfaces were *in situ* obtained by scraping with a diamond file in the sample preparation chamber below 1×10^{-10} Torr. Changes of the spectral feature due to the carbon and/or oxygen contamination have not been observed within 24 h and experiments were performed within 12 h after the surface cleaning. The energy of all spectra is defined with respect to E_F determined from the spectra of the fleshly evaporated Au film.

Polycrystalline $(La_{1-x}Ca_xO)Cu_{1-x}Ni_xS$ samples used for the UPS, IPES, and SRPES experiments were prepared by the solid-state reaction. Stoichiometric amount of La_2O_3, La_2S_3, CaO, CuS, and NiS powders were thoroughly mixed under an Ar atmosphere. La_2O_3 and CaO were preheated at 900 °C for 10 h to remove hydroxides and carbonates prior to mixing the starting materials. The mixture was pressed into a bar and the bar was sintered at 900 °C for 40 h in an evacuated ampoule with 10^{-5} Torr.

The grown samples were characterized by means of the x-ray powder diffraction (XRD), energy dispersive x-ray fluorescence spectroscopy (EDX), electrical resistivity, and scanning electron microscopy (SEM) experiments. Figure 2 shows the XRD patterns of the grown samples for $x=0$, 0.03, and 0.07 together with the calculation for $x=0$. One notices that all diffraction peaks are in agreement with the calculation and the grown samples have a single phase with the (LaO)AgS-type structure. No peak originating from impurities such as CuO is observed within an experimental accuracy. According to the XRD measurements using synchrotron radiation at SPring-8,[13] an amount of impurity phases in (LaO)CuS is less than 0.1%.

Real compositions of the constituent ions for the grown samples estimated by the EDX measurements are in agreement with the nominal values (x) within $\pm1\%$. The Ni and Cu $3p$ XPS measurements as described in Sec. III also indi-

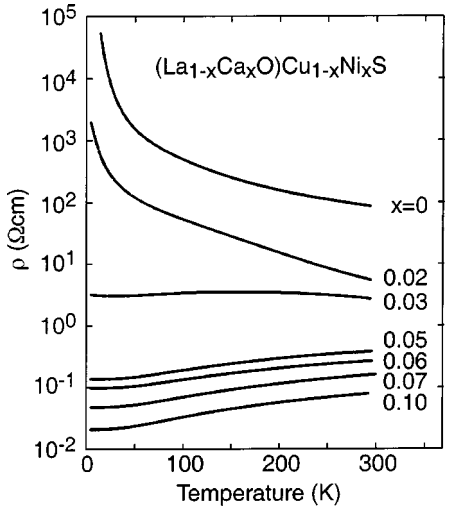

FIG. 3. Electrical resistivities of $(La_{1-x}Ca_xO)Cu_{1-x}Ni_xS$ $(0 \leqslant x \leqslant 0.10)$.

cate that the compositions are close to the x values (see Fig. 6). The x dependence of the electrical resistivity for $0 \leqslant x \leqslant 0.10$ shown in Fig. 3 is semiconductive for $x \leqslant 0.02$, metallic for $x \geqslant 0.04$ and the metal-semiconductor transition at $\sim$150 K for $x = 0.03$. This indicates that the Ca and Ni ions are indeed doped into the samples continuously and systematically with x.

Figure 4 shows the SEM images for $x = 0$, 0.03, and 0.07. From these images, one notices that the grown samples are composed of more or less large pieces with habits and they are homogeneous. In particular, a size of the pieces increases

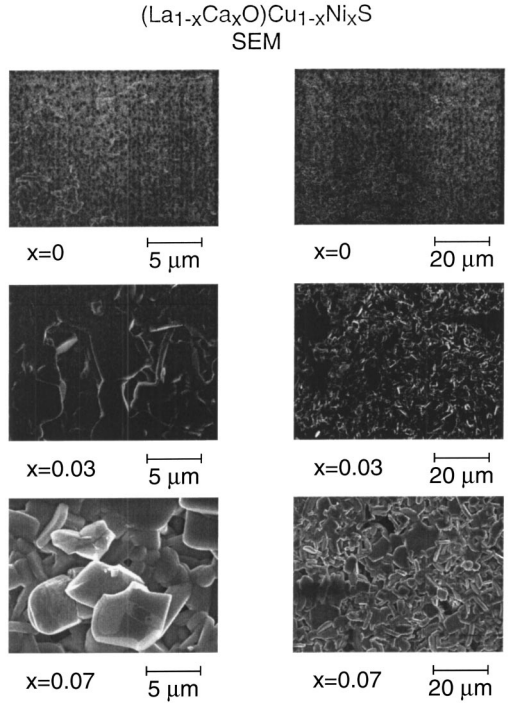

FIG. 4. SEM images of $(La_{1-x}Ca_xO)Cu_{1-x}Ni_xS$ with $x = 0$, 0.03, and 0.07.

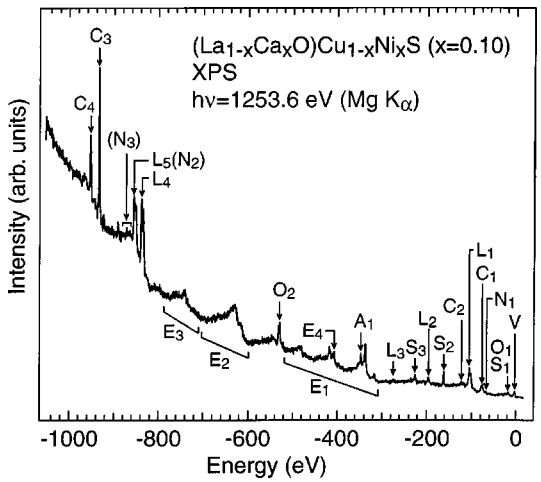

FIG. 5. The XPS spectrum of $(La_{0.90}Ca_{0.10}O)Cu_{0.90}Ni_{0.10}S$ measured with the Mg K_α line. Several arrows indicate structures due to the valence bands (V), La $4d$ (L_1), La $4p$ (L_2), La $4s$ (L_3), La $3d_{5/2}$ (L_4), La $3d_{3/2}$ (L_5), O $2s$ (O_1), O $1s$ (O_2), Cu $3p$ (C_1), Cu $3s$ (C_2), Cu $2p_{3/2}$ (C_3), Cu $2p_{1/2}$ (C_4), S $3s$ (S_1), S $2p$ (S_2), S $2s$ (S_3), Ni $3p$ (N_1), Ni $2p_{3/2}$ (N_2), and Ca $2p$ (A_1) states. The structures in the E_1, E_2, and E_3 regions originate from the Cu LMM, La MNN, and O KLL Auger electron emissions, respectively. The E_4 peak is also one of the Ni LMM Auger structures. An arrow with N_3 denotes the energy region of the Ni $2p_{1/2}$ states.

with x to the μm order, indicating that the Ca and Ni codoped systems crystallize more easily than (LaO)CuS.[14] Thus the samples used for the present experiments have enough high quality to measure the UPS, IPES, and SRPES spectra with respect to the crystal structure, composition, and homogeneity.

III. RESULTS AND DISCUSSION

Figure 5 depicts the XPS spectrum of $(La_{0.90}Ca_{0.10}O)Cu_{0.90}Ni_{0.10}S$ in the wide energy region. One notices that the several structures derived from the constituent elements are observed. The Cu $2p_{3/2}$- $(C_3$ in the figure) and $2p_{1/2}$- (C_4) derived peaks are observed at -933 and -953 eV, respectively. No remarkable satellite structure is found, and it is difficult to evaluate the satellite intensity ratio relative to main peak intensity due to the Cu $2p$ states, as done by Takano *et al.*[8] For the substituted elements, the weak structures due to the Ni $3p$ (N_1) and Ca $2p$ (A_1) states are detected at -68 and -347 eV, respectively. One of the Ni LMM Auger structures is also observed at -408 eV (E_4). On the other hand, the Ni $2p_{1/2}$ states are not clearly detected, the energy region of which is indicated by an arrow with N_3. The structure of the Ni $2p_{3/2}$ states (N_2) is overlapped with that of the La $3d_{3/2}$ states (L_5).

Also, as shown in Fig. 6(a), the SRPES spectrum of $(La_{1-x}Ca_xO)Cu_{1-x}Ni_xS$ with $x = 0.10$ in the Cu and Ni $3p$ regions clearly shows the structure due to the Ni $3p$ states, in comparison with that of (LaO)CuS $(x = 0)$. We have carried out the curve fitting for the experimental spectrum of $x = 0.10$. The background contribution is removed from the experimental spectrum, and the Gaussian functions are used

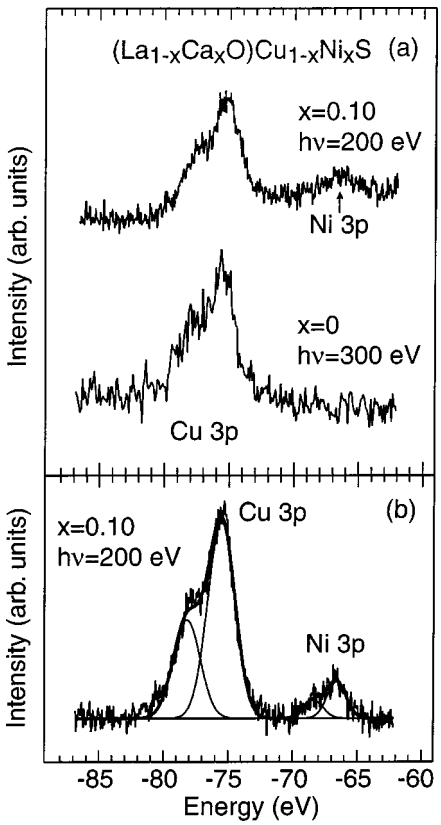

FIG. 6. (a) SRPES spectra of $(La_{1-x}Ca_xO)Cu_{1-x}Ni_xS$ with $x=0$ and 0.10 in the Cu and Ni $3p$ regions. (b) The SRPES spectrum fitted with the Gaussian functions for the Cu $3p_{3/2}$, Cu $3p_{1/2}$, Ni $3p_{3/2}$ and Ni $3p_{1/2}$ states.

for the $3p_{3/2}$ and $3p_{1/2}$ states of both Cu and Ni elements, where the intensity ratio of the $3p_{3/2}$ and $3p_{1/2}$ peaks is fixed to 2:1. Here, we neglect a lifetime broadening effect for simplicity. The curve fitting reproduces well the experimental result as shown in Fig. 6(b). The derived intensity of the Cu $3p$ peak relative to that of the Ni $3p$ peak is about 7.5. Taking into account the photoionization cross sections of the Cu and Ni $3p$ states at $h\nu=200$ eV,[15] the amount of the Ni elements is estimated to be ~12%, in good agreement with the nominal concentration.

Next, the UPS and SRPES spectra of (LaO)CuS are presented in Fig. 7. The UPS spectrum at $h\nu=21.2$ eV shows structures at ~ -1.5 (A), -3.2 (B), -5.0 (C), and -6 eV (D). With increasing $h\nu$ to 40.8 eV, structure B is enhanced as a prominent peak and structure D almost disappears. The other two structures, A and C, exhibit little change. In addition, one notices a clear structure at -9.5 eV (E), which is slightly observed in the UPS spectrum at $h\nu=21.2$ eV behind the background due to the secondary electrons. At $h\nu=200$ eV, peak B with shoulder A is observed as a prominent peak and component C is observed as a tail. Structure D disappears and structure E is slightly observed. The $h\nu$ dependence of the UPS and SRPES spectra are explained by the photoionization cross sections of the valence electron orbitals.[15] The valence bands are mainly composed of the Cu $3d$, S $3p$, and O $2p$ states. At $h\nu=21.2$ eV, the cross sections of these states are similar. With increasing $h\nu$ to 40.8 eV, that of the S $3p$ states rapidly decreases relative to the Cu $3d$ and O $2p$ states. For further increase of $h\nu$ to 200 eV, only the Cu $3d$ states contribute to the photoemission spectra; the ratios of the cross sections at $h\nu=200$ eV are $[\text{Cu } 3d]/[\text{O } 2p]\sim 14$ and $[\text{Cu } 3d]/[\text{S } 3p]\sim 15$. Accordingly, structures A, B, and C are ascribed to the Cu $3d$ states hybridized with the S $3p$ states and structure D to the O $2p$ states.

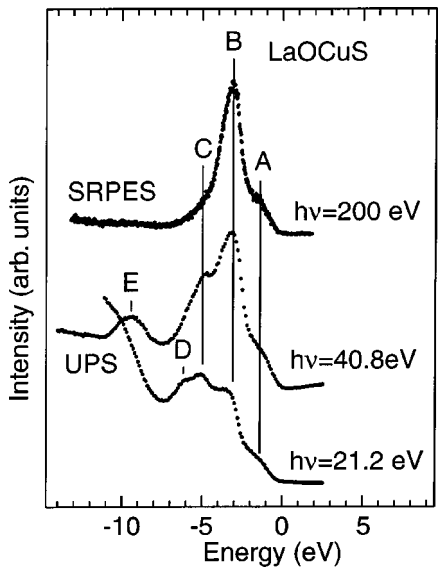

FIG. 7. UPS spectra measured at $h\nu=21.2$ and 40.8 eV, and SRPES spectrum at $h\nu=200$ eV of (LaO)CuS.

The Cu $3d$ states coordinated tetrahedrally by four S ions split into the triplet t_{2g} and doublet e_g states under the crystal field with T_d symmetry. From the symmetries of the wave functions, the t_{2g} states well hybridize with the S $3p$ states, while the e_g states have a nearly localized character. Therefore the structures A, B, and C are attributed to the Cu $3d$ $(t_{2g})-$S $3p$ antibonding states, nearly localized Cu $3d$ (e_g) states and Cu $3d$ $(t_{2g})-$S $3p$ bonding states, respectively. It should be noticed that the Cu $3d$ $(t_{2g})-$S $3p$ antibonding states mainly contribute to the top of the valence bands of (LaO)CuS, as predicted by the band-structure calculation.[1]

As for structure E around -9.5 eV, its origin cannot be specified clearly in the present stage. Structure E is also observed for all the Ca and Ni co-doped system $(La_{1-x}Ca_xO)Cu_{1-x}Ni_xS$ with the almost similar intensity and feature (see Fig. 9). The Cu $3d$-derived satellite structures are observed around -10 eV as clear double peaks in the photoemission spectra of CuO (Cu^{2+}),[16,17] while structure E in Fig. 7 is a single peak. Furthermore, since the Cu ion in the $(La_{1-x}Ca_xO)Cu_{1-x}Ni_xS$ compound is almost monovalent, as indicated by the Cu $2p$ XPS, SRPES (Fig. 8, shown later) and NMR experiments,[9] structure E is not attributable to the Cu $3d$ states. This is strongly supported from the photoemission result for (LaO)CuS that structure E almost disappears at $h\nu=200$ eV.

A bump around -9.5 eV is observed in the UPS spectra of polycrystalline $La_{1-x}Sr_xMnO_3$ also prepared by the solid-state reaction in case that the surface cleaning is insufficient.[18] If structure E is caused by some contamina-

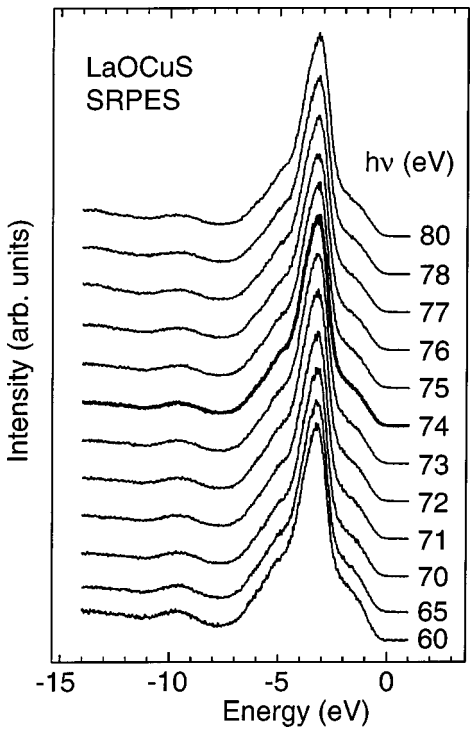

FIG. 8. $h\nu$ dependence of the SRPES spectra of (LaO)CuS including the Cu $3p$-$3d$ excitation region. The thick line is a spectrum taken near the Cu $3p$-$3d$ resonance.

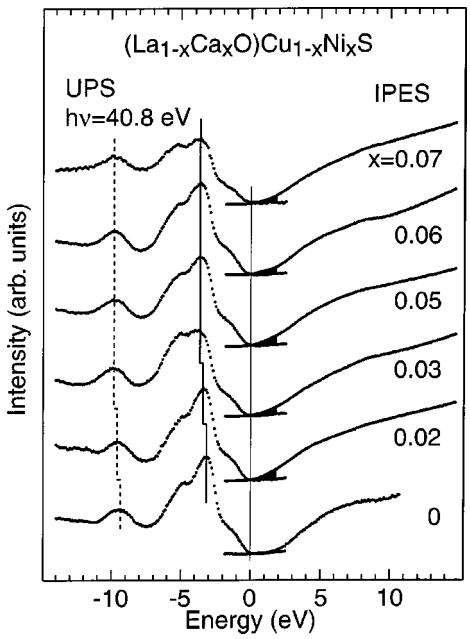

FIG. 9. A series of the UPS spectra measured at $h\nu=40.8$ eV and IPES spectra of $(La_{1-x}Ca_xO)Cu_{1-x}Ni_xS$ $(0\leqslant x\leqslant 0.07)$.

tions, these are intrinsically included in the grain boundary of the present samples, since the intensity and feature of structure E are independent of the surface cleaning by scraping. However, the grain boundary estimated to at most ~3% in area relative to the whole sample surface from the SEM image is too small to give rise to the clear structure. The main feature of the O $1s$ XPS spectrum of (LaO)CuS (not shown here) is a single peak and has no tail on the higher binding energy side, suggesting almost no contamination.[19] In addition, the C $1s$ peak is not observed in the XPS spectrum. It should again be noticed that an amount of the impurity phases in the grown samples is estimated to be at most 0.1% by means of the XRD measurements using synchrotron radiation.[13]

Recently, we have carried out the O $2p$-$1s$ emission experiments on (LaO)CuS in order to deduce the O $2p$ partial DOS in the valence bands.[20] Preliminary results indicate that the O $2p$ partial DOS is located at ~ -6 eV as a peak and structure E is not due to the O $2p$ states. In order to clarify the origin of structure E, the soft x-ray emission experiments in the La, S, and Cu core excitation region is in progress. For further discussion, the growth of the single crystal with high quality is also required necessarily.

In order to derive the Cu $3d$ contribution to the valence bands of (LaO)CuS, we have carried out the resonant photoemission experiments in the Cu $3p$-$3d$ excitation region (~74 eV). The experimental results are shown in Fig. 8. The SRPES spectra are measured at $h\nu$ from 60 to 80 eV including the Cu $3p$-$3d$ excitation region. All spectra are normalized to the monochromator output. The SRPES spectrum at $h\nu=74$ eV is indicated by a thick line. One notices no remarkable enhancement for the photoemission intensity in the Cu $3p$-$3d$ excitation region within an experimental accuracy. The resonance enhancement takes place as a result of the interference effect of the two processes of (i) $(3p)^6(3d)^n+h\nu\rightarrow(3p)^6(3d)^{n-1}+\varepsilon_d$ and (ii) $(3p)^6(3d)^n+h\nu\rightarrow(3p)^5(3d)^{n+1}\rightarrow(3p)^6(3d)^{n-1}+\varepsilon_d$, where ε_d represents an emitted $3d$ photoelectron. In case that the Cu atom exists in the compounds in the form of the Cu^{2+} ion, the resonance enhancement should take place in the $3d$ photoemission intensity, in particular, in that of the satellite structure at ~ -9.5 eV.[16] On the other hand, since the Cu $3d$ orbitals of the Cu^{1+} ion are fully occupied by electrons, the Cu $3p$-$3d$ excitation does not take place so much and, as a result, no resonant enhancement is observed. Actually, the Cu $3p$-$3d$ absorption is also not detected in the Cu $3p$-$3d$ excitation region in the present experiments. Therefore the Cu ion in (LaO)CuS is monovalent (Cu^{1+}, $3d^{10}$), in agreement with the result of the NMR study.[9] Also from the similar SRPES spectra of $(La_{0.90}Ca_{0.10}O)Cu_{0.90}Ni_{0.10}S$ (not shown here), the Cu ion in the Ca and Ni co-doped system remains monovalent, in consistent with the x-independent ^{63}Cu NMR shift.[9]

Now, we shall be concerned with the x dependence of the spectra of the Ca and Ni co-doped system $(La_{1-x}Ca_xO)Cu_{1-x}Ni_xS$. Figure 9 shows a series of UPS spectra measured at $h\nu=40.8$ eV together with IPES spectra of $(La_{1-x}Ca_xO)Cu_{1-x}Ni_xS$ $(0\leqslant x\leqslant 0.07)$. Energy is defined with respect to E_F of respective samples. E_F is close to the valence-band maximum (VBM) for the semiconductive region of $x\leqslant 0.03$, indicating that the Ca and Ni co-doped system is also the p-type semiconductor. Still for the metallic region ($x>0.03$), the DOS at E_F is substantially low and a clear Fermi edge is not observed in the UPS and IPES spectra. The low DOS at E_F at the Cu sites for the metallic region has also been confirmed from the analysis of the temperature

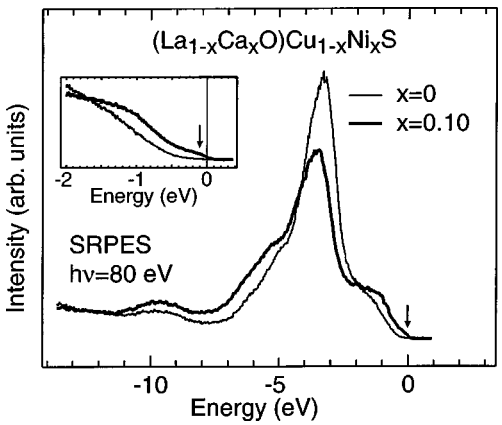

FIG. 10. SRPES spectra of $(La_{1-x}Ca_xO)Cu_{1-x}Ni_xS$ with $x=0$ and 0.10 measured at $h\nu=80$ eV. Spectra near E_F are shown in the inset. The finite DOS at E_F is observed for $x=0.10$ as indicated by a vertical arrow.

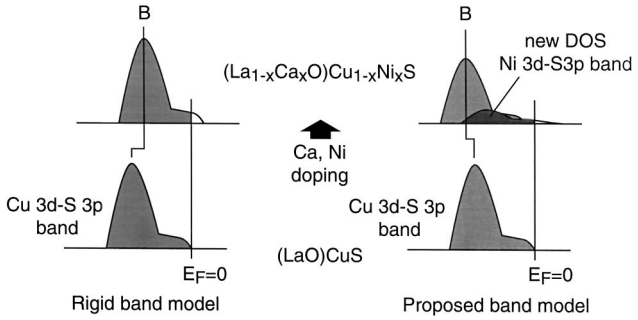

FIG. 11. Schematic band models for the valence-band electronic structure of $(La_{1-x}Ca_xO)Cu_{1-x}Ni_xS$. Left-hand side: rigid-band model. Right-hand side: proposed band model with the new DOS derived from the Ni $3d$ and S $3p$ states just above E_F of (LaO)CuS (see text for details).

dependence of the nuclear spin-lattice relaxation time of the ^{63}Cu NMR experiments.[9] Although the NMR experiments give information only on the Cu sites, the present results indicate that the contribution of the S $3p$ states to E_F is also low. One notices that the energy position of the main peak due to the nearly localized Cu $3d$ (e_g) states (structure B in Fig. 7) shifts to the deeper energy side from -3.2 eV for $x=0$ to -3.7 eV for $x=0.03$, and it keeps constant for $0.03 \leqslant x \leqslant 0.07$. A similar energy shift is observed in the structure around -9.5 eV (E in Fig. 7) as indicated by a dashed line in Fig. 9.

On the other hand, the IPES spectrum of (LaO)CuS ($x=0$) shows only a broad structure from 2 to 9 eV. The La $5d$ states together with the Cu $4s$ states contribute to this energy region. No distinct structure in the conduction bands is consistent with results of the band-structure calculations.[1] The energy separation between the VBM and conduction-band minimum (CBM), determined from the leading edges of the UPS and IPES spectra, is around 2.1 eV, which is small[21] in comparison with 3.1 eV derived from the photoluminescence data.[3] The basic feature of the IPES spectra is similar for $0 \leqslant x \leqslant 0.07$. It is noted that the CBM edge of the IPES spectrum becomes rapidly close to E_F for $x=0.02$, and become unchanged for $0.03 \leqslant x \leqslant 0.07$. The spectral weight in the energy region of 0–2 eV of the IPES spectra for $x \geqslant 0.02$ increases (shaded area in the figure), indicating the unoccupied states of some new DOS due to the co-doping effect.[23]

In order to see more clearly the Ca and Ni co-doping effect, we compare the SRPES spectra of $(La_{1-x}Ca_xO)Cu_{1-x}Ni_xS$ with $x=0$ and 0.10 measured at $h\nu=80$ eV in Fig. 10. For $x=0.10$, the intensity of the Cu $3d(e_g)$-derived main peak decreases, and the spectral weight transfers to the top 2-eV region and around -6 eV, in comparison with the spectrum of $x=0$. An inset shows the spectra near E_F. One notices the finite DOS at E_F in the spectra of $x=0.10$ compared with that of $x=0$, in consistent with the metallic behavior of $x=0.10$. Furthermore, the finite DOS at E_F is observed as a clear structure as indicated by a vertical arrow in the figure, suggesting the new DOS increases with x just above the Cu $3d(t_{2g})-$S $3p$ antibonding states of (LaO)CuS.

Based on the above experimental results, we discuss the band modification of (LaO)CuS induced by the Ca and Ni co-doping. In the $(La_{1-x}Ca_xO)Cu_{1-x}Ni_xS$ compounds, the ionic states of the elements have been considered to be La^{3+}, Ca^{2+}, O^{2-}, Cu^{1+}, Ni^{2+}, and S^{2-}. The nominal electron configurations of the Cu^{1+} and Ni^{2+} ions are $3d^{10}$ and $3d^8$, respectively. For (LaO)CuS, the Cu $3d-$S $3p$ bands are fully occupied, and E_F is located at the top of the Cu $3d-$S $3p$ hybridization bands, as shown schematically in Fig. 11, where "B" corresponds to the main peak B in Fig. 7. According to a rigid-band model (left-hand side in the figure), with increasing x, holes would be introduced simply into the Cu $3d-$S $3p$ bands. Then, E_F moves into the Cu $3d-$S $3p$ bands and the Cu $3d$ (e_g)-derived main peak becomes close to E_F, in contrast to the experimental results in Fig. 9, indicating that the rigid-band model is no longer valid for $(La_{1-x}Ca_xO)Cu_{1-x}Ni_xS$.

Next, we propose a simple band model taking into account the new DOS derived from the Ni $3d$ and S $3p$ states in $(La_{1-x}Ca_xO)Cu_{1-x}Ni_xS$. The Ni^{2+} $3d$ bands are expected to be shallower than the Cu^{1+} $3d$ bands, since the $3d$ electron number occupying the $3d$ bands is smaller for Ni^{2+} ions than for Cu^{1+} ions. The Ni $3d$ states also hybridize with the S $3p$ states and the Ni $3d-$S $3p$ antibonding states may appear as the new DOS at the higher energy side of E_F of (LaO)CuS, as shown at the right-hand side of Fig. 11. Holes are doped into this new DOS and E_F of $(La_{1-x}Ca_xO)Cu_{1-x}Ni_xS$ becomes higher than that of (LaO)CuS, leading to the energy shift of the Cu $3d$ (e_g)-derived main peak away from E_F. The rapid shift of the CBM edge with x in the IPES spectra is also understood as the unoccupied states of these new DOS.[23] This proposed band model thus explains qualitatively the observed energy shift of the Cu $3d$ (e_g)-derived peak, as well as the clear structure near E_F in the SRPES spectrum of $x=0.10$ as indicated by a vertical arrow in Fig. 10. Here, the Ca^{2+} ions play an important role to compensate a charge deviation in $[Cu_{1-x}Ni_xS]^{(1-x)-}$ layers by the neighboring $[La_{1-x}Ca_xO]^{(1-x)+}$ layers in order to keep the neutrality of the material. Since the Ca-derived states are expected to

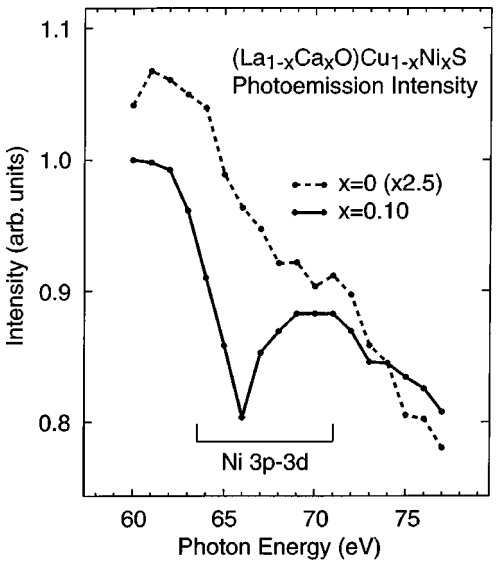

FIG. 12. The integrated photoemission intensities in the top 0.5-eV region in the valence bands of $(La_{1-x}Ca_xO)Cu_{1-x}Ni_xS$ with $x=0.10$ in the Ni $3p$-$3d$ excitation region (solid line), in comparison with the intensities in the top 1.0-eV region of (LaO)CuS (dotted line). The photo-emission intensities are calibrated by the monochromator output and normalized using the intensities at -0.5 eV of the photoemission spectra at $h\nu=60$ eV.

show up in the energy region much higher than the CBM, they are not shown in Fig. 11.

In order to clarify whether the new DOS near E_F in the SRPES spectrum of $(La_{1-x}Ca_xO)Cu_{1-x}Ni_xS$ with $x=0.10$ is due to the Ni $3d$ states, we have measured the resonant photoemission spectra in the Ni $3p$-$3d$ excitation region ($\sim$65 eV). The SRPES spectra are normalized to the monochromator output. Because the $h\nu$ dependence of the photoemission intensities near E_F is substantially weak, we plot the integrated intensity in the top 0.5-eV region in the valence bands as a function of $h\nu$. The result is shown in Fig. 12 by a solid line, in comparison with the intensities in the top 1.0-eV region of (LaO)CuS by a dotted line. One notices a clear resonance feature in the spectrum of $x=0.10$. From $h\nu=60$ eV, the integrated intensity gradually decreases with $h\nu$, and reaches to a minimum at $h\nu=66$ eV. The resonance enhancement takes place at $h\nu=66-70$ eV. After that, the intensity again decreases with $h\nu$. The line shape is close to the Fano type with a q parameter of nearly zero.[24,25] Such a resonance behavior is often observed for Ni compounds.[26] The experimental results indicate that the new DOS is indeed due to the Ni $3d$ states and support the proposed band model in Fig. 11.

Finally, we should notice a difference between the present results for (LaO)CuS and those for the Sr singly doped system $(La_{0.95}Sr_{0.05}O)CuS$ measured by Inoue *et al.*[1] The characteristic structures A, B, C, and D in the UPS and XPS spectra for $(La_{0.95}Sr_{0.05}O)CuS$ are observed at -1.9, -3.6, -5.3, and -6.3 eV, respectively, which are shallower than those of (LaO)CuS by $\sim$0.4 eV. Although such an energy shift is comparable to the value of $\sim$0.5 eV for the Ca and Ni co-doped system $(La_{1-x}Ca_xO)Cu_{1-x}Ni_xS$ with $x\geqslant 0.03$, there is a remarkable difference in the photoemission intensities just below E_F. The photoemission intensities for $(La_{0.95}Sr_{0.05}O)CuS$ is substantially low in the top 0.4-eV region below E_F (see Fig. 2 in Ref. 1), in contrast to the relatively high intensities for all $(La_{1-x}Ca_xO)Cu_{1-x}Ni_xS$ (Figs. 9 and 10). Such results can be attributed to the formation of the impurity levels in the band gap in the Sr-doped system, which may be derived from the Sr ions or some crystalline imperfections, and located at $\sim$0.4 eV above the VBM. Taking into account the fact that $(La_{0.95}Sr_{0.05}O)CuS$ is metallic with the resistivity of the order of 1 Ω cm,[7] the actual Sr concentration measured by Inoue *et al.* may be slightly lower than the nominal concentration of $x=0.05$. In any way, we would like to emphasize the difference between the single-doping and co-doping effects on the valence-band electronic structure of (LaO)CuS. The valence bands of (LaO)CuS can easily be modified for the co-doped system but hardly for the singly doped system, since the replaced elements for the Cu ions would produce new DOS near the top of the valence bands.

IV. SUMMARY

We have investigated electronic structure of the transparent p-type (LaO)CuS and the Ca and Ni co-doped system $(La_{1-x}Ca_xO)Cu_{1-x}Ni_xS$ ($x\leqslant 0.10$), and found that the simultaneous substitution of the Ca and Ni ions for the La and Cu ions produces the Ni $3d$ and S $3p$-derived new DOS near E_F, which is essential for metallic behavior for $x\geqslant 0.03$. From this result, more drastic change of the band structure is expected for Co, Fe, and/or Mn substituted systems for Cu ions. The magnetic element dopings to (LaO)CuS would also lead to the fabrication of new transparent magnetic semiconductors. The solid solution between p-type (LaO)CuS and n-type (LaO)AgS,[5] with nearly the same in-plane lattice constant, would be a candidate of homogenous p-n junctions.

ACKNOWLEDGMENTS

The authors are grateful to Y. Hanaoka and K. Yoshikawa for their experimental support and to Dr. T. Saito for valuable discussions. The synchrotron radiation experiments have been done under the approval of HSRC (Proposal No. 01-A-21).

*Present address: Hiroshima Synchrotron Radiation Center, Hiroshima University, Kagamiyama 2-313, Higashi-Hiroshima 739-8526, Japan.

[1] S. Inoue, K. Ueda, and H. Hosono, Phys. Rev. B **64**, 245211 (2001).

[2] K. Ueda, S. Inoue, H. Hosono, N. Sarukura, and M. Hirano, Appl. Phys. Lett. **78**, 2333 (2001).

[3] K. Ueda, S. Inoue, S. Hirose, H. Kawazoe, and H. Hosono, Appl. Phys. Lett. **77**, 2701 (2000).

[4] M. Palazzi, C. Carcaly, and J. Flahaut, J. Solid State Chem. **35**,

150 (1980).
[5] K. Ishikawa, S. Kinoshita, Y. Suzuki, S. Matsuura, T. Nakanishi, M. Aizawa, and Y. Suzuki, J. Electrochem. Soc. **138**, 1166 (1991).
[6] K. Sekizawa, Y. Takano, K. Mori, and K. Yahagi, Czech. J. Phys. **46**, 1943 (1996).
[7] Y. Takano, K. Yahagi, and K. Sekizawa, Physica B **206&207**, 764 (1995).
[8] Y. Takano, K. Mori, K. Koizumi, H. Ozaki, and K. Sekizawa, J. Alloys Compd. **275–277**, 447 (1998).
[9] Y. Furukawa, S. Ikeda, K. Kumagai, K. Mori, Y. Takano, and K. Sekizawa, Phys. Rev. B **62**, 15 598 (2000).
[10] K. Yokoyama, K. Nishihara, K. Mimura, Y. Hari, M. Taniguchi, Y. Ueda, and M. Fujisawa, Rev. Sci. Instrum. **64**, 87 (1993).
[11] Y. Ueda, K. Nishihara, K. Mimura, Y. Hari, M. Taniguchi, and M. Fujisawa, Nucl. Instrum. Methods Phys. Res. A **330**, 140 (1993).
[12] M. Taniguchi and J. Ghijsen, J. Synchrotron Radiat. **5**, 1176 (1998).
[13] Y. Kuroiwa *et al.* (unpublished).
[14] K. Takase *et al.* (unpublished).
[15] J. J. Yeh and I. Lindau, At. Data Nucl. Data Tables **32**, 1 (1985).
[16] M. R. Thuler, R. L. Benbow, and Z. Hurych, Phys. Rev. B **26**, 669 (1982).
[17] F. Parmigiani and L. Sangaletti, J. Electron Spectrosc. Relat. Phenom. **107**, 49 (2000).
[18] T. Saitoh, A. E. Bocquet, T. Mizokawa, H. Namatame, A. Fujimori, M. Abbate, Y. Takeda, and M. Takano, Phys. Rev. B **51**, 13 942 (1995).
[19] The structure, the origin of which is not clear, is observed on the lower binding-energy side by 3 eV of the O 1*s* main peak.
[20] H. Sato *et al.* (unpublished).
[21] The energy separation of the VBM and CBM derived from the UPS and IPES spectra is often smaller than the band-gap energy (Ref. 22) due to the tail to the lower photon energy of a response curve, centered at 9.43 eV with a full width at half maximum of 0.47 eV, for the band-pass photon detector used in the IPES experiments (Refs. 10 and 11).
[22] H. Sato, M. Taniguchi, K. Mimura, S. Senba, H. Namatame, and Y. Ueda, Phys. Rev. B **61**, 10 622 (2000).
[23] The gradual increase of the inverse-photoemission intensity toward the higher energy side would be due to the inelastic scattering of the injected electrons.
[24] U. Fano, Phys. Rev. **124**, 1866 (1961).
[25] A. Shibatani and Y. Toyozawa, J. Phys. Soc. Jpn. **25**, 335 (1968).
[26] A. Fujimori, K. Mamiya, T. Mizokawa, T. Miyadai, T. Sekiguchi, H. Takahashi, N. Mori, and S. Suga, Phys. Rev. B **54**, 16 329 (1996).